Measurement of the Double-Beta Decay Half-life of ^{136}Xe in KamLAND-Zen

A. Gando,[1] Y. Gando,[1] H. Hanakago,[1] H. Ikeda,[1] K. Inoue,[1,2] R. Kato,[1] M. Koga,[1,2] S. Matsuda,[1] T. Mitsui,[1] T. Nakada,[1] K. Nakamura,[1,2] A. Obata,[1] A. Oki,[1] Y. Ono,[1] I. Shimizu,[1] J. Shirai,[1] A. Suzuki,[1] Y. Takemoto,[1] K. Tamae,[1] K. Ueshima,[1] H. Watanabe,[1] B.D. Xu,[1] S. Yamada,[1] H. Yoshida,[1] A. Kozlov,[2] S. Yoshida,[3] T.I. Banks,[4] J.A. Detwiler,[4] S.J. Freedman,[2,4] B.K. Fujikawa,[2,4] K. Han,[4] T. O'Donnell,[4] B.E. Berger,[5] Y. Efremenko,[2,6] H.J. Karwowski,[7] D.M. Markoff,[7] W. Tornow,[7] S. Enomoto,[2,8] and M.P. Decowski[2,9]

(The KamLAND-Zen Collaboration)

[1]*Research Center for Neutrino Science, Tohoku University, Sendai 980-8578, Japan*
[2]*Institute for the Physics and Mathematics of the Universe, Tokyo University, Kashiwa 277-8568, Japan*
[3]*Graduate School of Science, Osaka University, Toyonaka, Osaka 560-0043, Japan*
[4]*Physics Department, University of California, Berkeley, and Lawrence Berkeley National Laboratory, Berkeley, California 94720, USA*
[5]*Department of Physics, Colorado State University, Fort Collins, Colorado 80523, USA*
[6]*Department of Physics and Astronomy, University of Tennessee, Knoxville, Tennessee 37996, USA*
[7]*Triangle Universities Nuclear Laboratory, Durham, North Carolina 27708, USA and Physics Departments at Duke University, North Carolina Central University, and the University of North Carolina at Chapel Hill*
[8]*Center for Experimental Nuclear Physics and Astrophysics, University of Washington, Seattle, Washington 98195, USA*
[9]*Nikhef and the University of Amsterdam, Science Park, Amsterdam, the Netherlands*

(Dated: January 17, 2016)

We present results from the KamLAND-Zen double-beta decay experiment based on an exposure of 77.6 days with 129 kg of ^{136}Xe. The measured two-neutrino double-beta decay half-life of ^{136}Xe is $T^{2\nu}_{1/2} = 2.38 \pm 0.02(\mathrm{stat}) \pm 0.14(\mathrm{syst}) \times 10^{21}$ yr, consistent with a recent measurement by EXO-200. We also obtain a lower limit for the neutrinoless double-beta decay half-life, $T^{0\nu}_{1/2} > 5.7 \times 10^{24}$ yr at 90% C.L.

PACS numbers: 23.40.-s, 21.10.Tg, 14.60.Pq

arXiv:1201.4664v1 [hep-ex] 23 Jan 2012

Majorana neutrinos are a natural feature of many high-energy theoretical models. However, the only viable experimental probe of this property at present is neutrinoless double-beta ($0\nu\beta\beta$) decay. Observation of this lepton-number violating nuclear process would definitively establish the Majorana nature of the neutrino, and would be a profound discovery [1]. In addition, since the rate of this process increases with the square of the effective neutrino mass $\langle m_{\beta\beta}\rangle \equiv \left|\Sigma_i U^2_{ei} m_{\nu_i}\right|$, its measurement would provide information on the absolute neutrino mass scale. Searches for $0\nu\beta\beta$ decay have been invigorated by recent measurements of neutrino mass splittings by oscillation experiments, which require at least one neutrino mass above ∼50 meV [2]. This scale is within the reach of present-day efforts.

Determining $\langle m_{\beta\beta}\rangle$ from a $0\nu\beta\beta$ decay half-life requires knowledge of the decay's phase-space factor ($G^{0\nu}$) and nuclear matrix element ($M^{0\nu}$). $G^{0\nu}$ can be calculated exactly, but to date all estimations of $M^{0\nu}$ must rely on model-based approximations possessing difficult-to-quantify uncertainties. The two-neutrino double-beta ($2\nu\beta\beta$) decay half-life, if known, can be used to constrain some relevant model parameters, reducing some sources of uncertainty [3, 4]. The first direct measurement of the $2\nu\beta\beta$ decay half-life of ^{136}Xe, recently reported by EXO-200 [5], was significantly below previously published lower limits [6, 7]. This Letter on the first results from the KamLAND-Zen (KamLAND Zero-Neutrino Double-Beta Decay) experiment reports a new measurement of the ^{136}Xe $2\nu\beta\beta$ decay half-life, as well as improved limits on $0\nu\beta\beta$ mode. The data presented were collected between October 12, 2011, and January 2, 2012.

KamLAND-Zen (Fig. 1) is a modification of the existing KamLAND detector carried out in the summer of 2011. The $\beta\beta$ source/detector is 13 tons of Xe-loaded liquid scintillator (Xe-LS) contained in a 3.08-m-diameter spherical inner balloon (IB). The IB is constructed from 25-μm-thick transparent nylon film and is suspended at the center of the KamLAND detector [8] by 12 film straps of the same material. The IB is surrounded by 1 kton of liquid scintillator (LS) contained in a 13-m-diameter spherical outer balloon (OB) made of 135-μm-thick nylon/EVOH (ethylene vinyl alcohol copolymer) composite film. The outer LS is 0.10% less dense than the Xe-LS and acts as an active shield for external γ's and as a detector for internal radiation from the Xe-LS or IB. The Xe-LS consists of 82% decane and 18% pseudocumene (1,2,4-trimethylbenzene) by volume, 2.7 g/liter of the fluor PPO (2,5-diphenyloxazole), and (2.52 ± 0.07) wt% of enriched xenon gas, as measured by gas chromatography. The isotopic abundances in the enriched xenon were measured by residual gas analyzer to be $(90.93 \pm 0.05)\%$ ^{136}Xe and $(8.89 \pm 0.01)\%$ ^{134}Xe. The light yield of the Xe-LS is 3% lower than that of the LS. Buffer oil (BO) between the OB and an 18-m-diameter spherical stainless-steel containment tank (SST) shields the LS from external radiation. Scintillation light is recorded by 1,325 17-inch and 554 20-inch photomultiplier tubes (PMTs) mounted on the SST, providing 34% solid-angle coverage. The SST is surrounded by a 3.2 kton water-Cherenkov detector. Details of the KamLAND detector are given in [8].

The data acquisition system (DAQ) is triggered when 70 or more 17-inch PMTs are hit (primary trigger), which corresponds to a threshold of ∼0.4 MeV. The signals on all hit

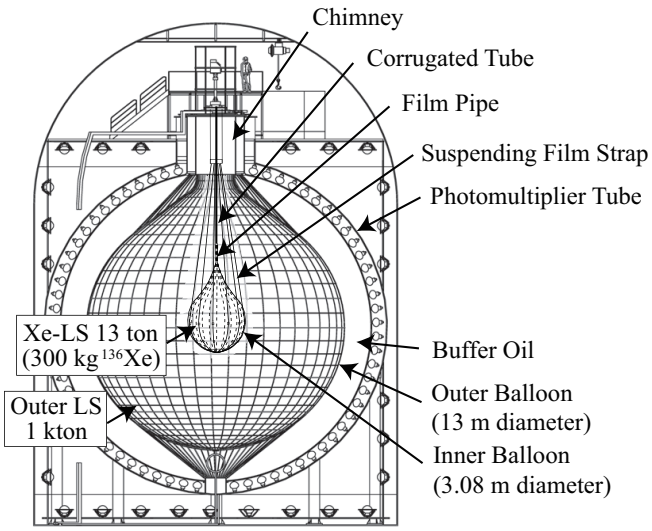

FIG. 1: Schematic diagram of the KamLAND-Zen detector.

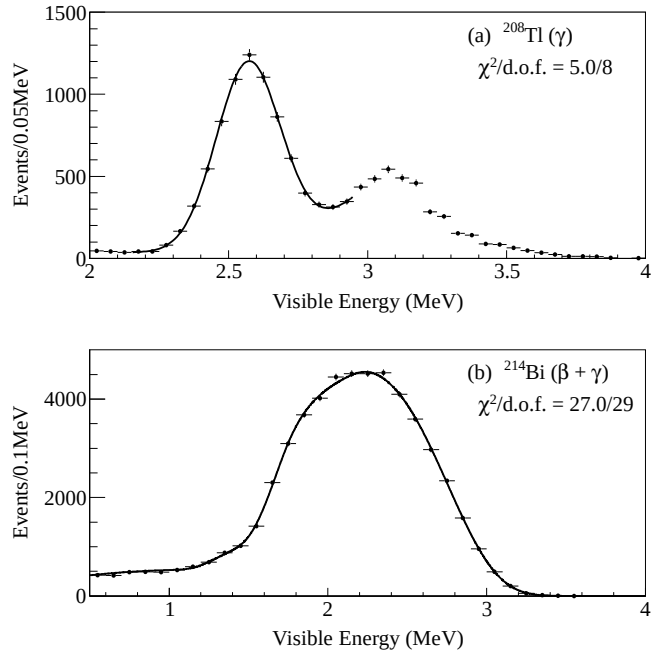

FIG. 2: Visible energy distributions of (a) γ's from the ^{208}Tl calibration source and (b) ^{214}Bi ($\beta + \gamma$'s) decays in the Xe-LS. The lines indicate the best-fits to the analytical spectral models with the resolution and energy scale parameters floating.

PMTs are digitized for ∼200 ns for offline analysis. After each primary trigger the threshold is lowered to ∼0.25 MeV for 1 ms to study sequential decays. The scintillation light from the two coincident e^- produced by ^{136}Xe $\beta\beta$ decay cannot be separated, so only their summed energy is observed. For hypothetical $0\nu\beta\beta$ decays, the sum is always 2.458 MeV (Q-value of the ^{136}Xe $\beta\beta$ decay) [9], while for the $2\nu\beta\beta$ decays the sum has a continuous spectrum up to the Q-value.

Event energy is estimated from the number of observed photoelectrons (p.e.) after correcting for PMT gain variation and solid angle, shadowing, and transparency of detector materials. The corrections depend on the event vertex, which is estimated from the PMT hit times. The vertex resolution is estimated from radial distributions of radioactive contaminants (see Fig. 3) to be $\sim 15\ \mathrm{cm}/\sqrt{E(\mathrm{MeV})}$. The energy response is calibrated with γ's from a ^{208}Tl ($\mathrm{ThO_2W}$) source, ^{214}Bi ($\beta + \gamma$'s) from ^{222}Rn ($\tau = 5.5$ day) introduced during detector modification, and 2.225 MeV γ's from spallation neutrons capture on protons.

Fig. 2(a) shows the energy spectrum obtained when the $\mathrm{ThO_2W}$ source, contained in a ∼5-mm-thick lead capsule, was deployed close to the outer surface of the IB. The most intense peak is due to the primary γ of ^{208}Tl (2.614 MeV). The less intense peak near ∼3.1 MeV is from multiple-γ cascades of ^{208}Tl. According to Monte Carlo (MC) studies, the degradation of the primary γ inside the source is negligible, and the distribution around the primary peak can be described by a gaussian and a third-order polynomial. The mean and width of the gaussian are relatively insensitive to the polynomial parameters. The resultant energy resolution at 2.614 MeV is $(6.6 \pm 0.3)\%/\sqrt{E(\mathrm{MeV})}$. The parameters of a detector energy response model describing effects from scintillator quenching and Cherenkov light production are constrained to reproduce the 2.614 MeV ^{208}Tl peak position and the spectral shape of ^{214}Bi events (Fig. 2(b)). The systematic variation of the energy reconstruction over the Xe-LS volume is less than 1.0%, and the detector energy response is stable to within 1.0% during the data set.

Candidate $\beta\beta$ decay events are selected by performing the following series of cuts: (i) The reconstructed vertex must be within 1.2 m of the detector center, defining the fiducial volume (FV). (ii) Muon events and events occurring within 2 ms after muons are eliminated. (iii) A coincidence cut eliminates sequential events that occur within 3 ms of each other; this removes $(99.97 \pm 0.01)\%$ of ^{214}Bi-^{214}Po (τ=237 μs) decays. This cut is augmented with a secondary cut, aimed at identifying sequential ^{212}Bi-^{212}Po (τ=0.4 μs), which exploits detailed PMT waveform data to identify coincidences within a single ∼200-ns-long DAQ event window. The ^{212}Bi-^{212}Po rejection efficiency is $(89 \pm 2)\%$. The dead time introduced by the coincidence cuts is less than ∼0.1%. (iv) A background mainly from reactor $\overline{\nu}_e$'s producing a delayed coincidence of positrons and neutron capture γ's is rejected by requiring event time separation greater than 1 ms. (iv) Finally, candidates must pass a vertex-time-charge (VTQ) test designed to filter out noise events. The test compares the observed PMT charge and hit-time distributions to those expected based on the reconstructed vertex [10]. The VTQ cut is tuned using KamLAND calibration data and reduces the selection efficiency by less than 0.1%. The total livetime after all cuts is 77.6 days. The energy spectrum of $\beta\beta$ decay candidates is shown in Fig. 4.

Backgrounds to the $\beta\beta$ decay study fall into three categories: those external to the Xe-LS, mainly from the IB material; those from residual radioactive impurities in the Xe-LS; and spallation backgrounds. From a spectral analysis of

events which reconstruct close to the IB boundary, we find that the activity in the energy region $1.2 < E < 2.0$ MeV ($2\nu\beta\beta$ window) is dominated by ^{134}Cs ($\beta + \gamma$); in the region $2.2 < E < 3.0$ MeV ($0\nu\beta\beta$ window), the spectrum is consistent with ^{214}Bi ($\beta + \gamma$) decays. The observed surface activity ratio of ^{134}Cs to ^{137}Cs (0.662 MeV γ) is consistent with contamination by fallout from the Fukushima-I reactor accident in March 2011. The FV cut is performed to mitigate the background from the IB material; the remaining IB background inside the FV is estimated by fitting Monte-Carlo-generated event radial distributions to the data. Fig. 3 shows the event density as a function of the cubed radius from the IB center for the two energy ranges, along with fits to the MC distributions. In the $2\nu\beta\beta$ window we fit for a $2\nu\beta\beta$ source uniformly distributed in the Xe-LS and a ^{134}Cs source uniformly distributed on the IB. In the $0\nu\beta\beta$ window we show the best-fits for a ^{214}Bi source uniformly distributed on the IB and either a $0\nu\beta\beta$-like source or a 2.6 MeV γ source uniformly distributed in the Xe-LS. The radial distribution offers no discrimination between these event types.

Assuming secular equilibrium, the residual ^{238}U and ^{232}Th concentrations internal to the Xe-LS are estimated to be $(3.5 \pm 0.6) \times 10^{-16}$ g/g and $(2.2 \pm 0.3) \times 10^{-15}$ g/g, respectively, based on sequential decays of ^{214}Bi-^{214}Po and ^{212}Bi-^{212}Po. Since equilibrium may be broken by introduction of contaminants during detector modification, the Bi-Po studies are only used to estimate internal background from the ^{222}Rn-^{210}Pb subchain of the ^{238}U series, and from the ^{228}Th-^{208}Pb subchain of the ^{232}Th series; other decays in both series are treated as unconstrained backgrounds. We note the well-known 2.614 MeV γ from ^{208}Tl (β^- decay, $Q = 5.00$ MeV) in the ^{232}Th series is not a serious background for the $0\nu\beta\beta$ decay search because of detection of the coincident β/γ in the surrounding active LS [11].

Spallation neutrons are tagged by coincidence of neutron capture γ's with preceding muons. We expect capture on protons (2.225 MeV), ^{12}C (4.946 MeV), ^{136}Xe (4.026 MeV), and ^{134}Xe (6.364 MeV), with fractions 0.994, 0.006, 9.5×10^{-4}, and 9.4×10^{-5}, respectively. We find no candidate ^{136}Xe or ^{134}Xe neutron capture candidates in the data set. ^{137}Xe (β^-, $\tau = 5.5$ min, $Q = 4.17$ MeV) from neutron capture on ^{136}Xe is a potential $0\nu\beta\beta$ background, but the expected production rate is negligible, $\sim 2.9 \times 10^{-3}$ (ton·day)$^{-1}$, where ton is a unit of Xe-LS mass. Production rates of light nuclei by spallation of carbon are calculated from spallation yields previously measured in KamLAND [8]. We observe a (13 ± 6)% increase in the spallation neutron flux in the Xe-LS relative to the outer LS, from which we assess a 19% systematic uncertainty on the calculated spallation yields. Events from decays of ^{11}C (β^+, $\tau = 29.4$ min, $Q = 1.98$ MeV) and ^{10}C (β^+, $\tau = 27.8$ s, $Q = 3.65$ MeV) dominate the contributions from spallation backgrounds. We expect rates of 1.11 ± 0.28 (ton·day)$^{-1}$ and $(2.11 \pm 0.44) \times 10^{-2}$ (ton·day)$^{-1}$ from ^{11}C and ^{10}C, respectively. The ^{11}C/^{10}C background can be reduced by a triple-coincidence tag of a muon, a neutron, and the ^{11}C/^{10}C decay. This is not pursued in the current analysis. We found no past experimental data for muon spallation of xenon. With the present data, we find the event rates

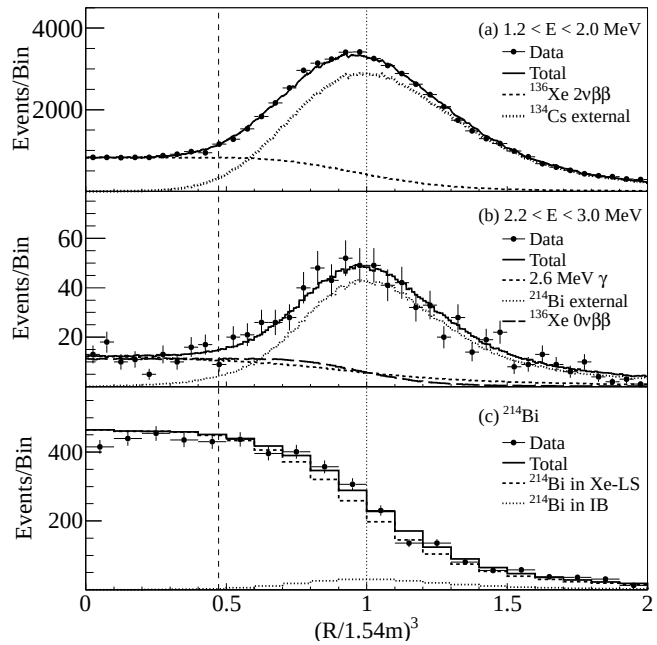

FIG. 3: R^3 vertex distribution of candidate events for (a) $1.2\ \mathrm{MeV} < E < 2.0\ \mathrm{MeV}$ and (b) $2.2\ \mathrm{MeV} < E < 3.0\ \mathrm{MeV}$. The curves show the best-fit model components: (a) $2\nu\beta\beta$ (dashed) and ^{134}Cs (dotted); (b) 2.6 MeV γ's (dashed) and ^{214}Bi (dotted), the long-dashed curve is for $0\nu\beta\beta$ instead of γ's. (c) ^{214}Bi events from Xe-LS (dashed) and IB (dotted). The vertical lines show the fiducial radius of 1.2 m (dashed) and the IB radius (dotted).

in the energy ranges for $1.2\ \mathrm{MeV} < E < 2.0\ \mathrm{MeV}$ and $2.2\ \mathrm{MeV} < E < 3.0\ \mathrm{MeV}$ from isotopes with lifetimes of less than 100 s associated with muons depositing more than $\sim$3 GeV in the detector (so-called showering muons) are less than 0.3 (ton·day)$^{-1}$and 0.02 (ton·day)$^{-1}$ at 90% C.L., respectively.

Care has to be taken for backgrounds that produce a peak close to the $0\nu\beta\beta$ decay energy (2.458 MeV), particularly ones which may have been introduced during detector modification or may be induced by muon spallation. We searched all isotopes in the ENSDF database [12] for sources with a peak structure between 2.4 and 2.8 visible-MeV. For all tabulated decay chains we calculate the visible energy spectrum, accounting for the time structure of the chain and pile-up in the DAQ event window, and apply the non-linear detector energy response model to all individual decay secondaries of each branch. Considering only nuclei with decay ancestor lifetimes longer than 30 days, we identify $^{110\mathrm{m}}$Ag (β^- decay, $\tau = 360$ day, $Q = 3.01$ MeV), ^{88}Y (EC decay, $\tau = 154$ day, $Q = 3.62$ MeV), ^{208}Bi (EC decay, $\tau = 5.31 \times 10^5$ yr, $Q = 2.88$ MeV), and ^{60}Co (β^- decay, $\tau = 7.61$ yr, $Q = 2.82$ MeV) as potential background sources. Observation of ^{134}Cs/^{137}Cs on the IB raises the plausibility of contamination of detector materials by Fukushima fallout, which include $^{110\mathrm{m}}$Ag. One assay of soil samples taken near the IB production facility reveal evidence of $^{110\mathrm{m}}$Ag. Although ^{88}Y, ^{208}Bi, and ^{60}Co are not detected near

Fukushima or our soil samples, we conservatively consider them to be possible backgrounds. Except for ^{208}Bi, these long-lived background candidates can be also produced from xenon spallation by cosmic-rays when materials were above-ground, but the rate estimations are difficult. Broadening the search to include shorter-lived nuclei ($100\ \mathrm{s} < \tau < 30\ \mathrm{day}$) possibly supported by muon spallation in the detector, we found that the production of candidate parents with mass numbers below ^{136}Xe is stringently constrained by comparing production cross sections in [13].

Nominally, the 1.2-m-radius FV corresponds to 0.438 ± 0.005 of the total Xe-LS volume ($16.51 \pm 0.17\ \mathrm{m}^3$), or 129 kg of ^{136}Xe. The fiducial volume fraction may also be estimated from the fraction of ^{214}Bi events which reconstruct within 1.2-m of the IB center compared to the total number in the entire Xe-LS volume after subtraction of the IB surface contribution. The result is $0.423 \pm 0.007(\mathrm{stat}) \pm 0.004(\mathrm{syst})$ (Fig. 3(c)). The difference in these estimates is taken as a measure of the systemic error on the vertex-defined FV. Combining the errors, we obtain a 5.2% systematic error on the fiducial volume. The total systematic uncertainty on the $\beta\beta$ decay half-life measurement is 5.9%, coming from the quadrature sum of the fiducial volume (5.2%), enrichment of ^{136}Xe (0.05%), Xe concentration (2.8%), detector energy scale (0.3%), and Xe-LS edge effect (0.06%).

The ^{136}Xe $2\nu\beta\beta$ and $0\nu\beta\beta$ decay rates are estimated from a likelihood fit to the binned energy spectrum of the selected candidates between 0.5 MeV and 4.8 MeV. The ^{136}Xe $2\nu\beta\beta$ decay spectrum shape from [14] is used. The contributions from major backgrounds in the Xe-LS, such as ^{85}Kr, ^{40}K, non-equilibrium ^{210}Bi, and the ^{238}U-^{222}Rn and ^{232}Th-^{224}Ra decay chains, are free parameters and are left unconstrained in the fit. The contributions from the ^{222}Rn-^{210}Pb and ^{228}Th-^{208}Pb chains, ^{11}C, and ^{10}C are allowed to vary but are constrained by their independent measurements. Residual IB-surface backgrounds in the FV are constrained by the radial distribution study. The parameters of the detector energy response model are floated but are constrained to reproduced the ^{208}Tl source and ^{222}Rn-induced ^{214}Bi data. Potential backgrounds from fallout nuclei with half-lives longer than 30 days found in ex-situ measurements of soil or ocean samples around Fukushima, namely ^{137}Cs, ^{134}Cs, $^{110\mathrm{m}}$Ag, $^{129\mathrm{m}}$Te, ^{95}Nb, ^{90}Y (from ^{90}Sr), and ^{89}Sr, as well as potential $0\nu\beta\beta$ backgrounds found in the ENSDF search (^{88}Y, ^{208}Bi, and ^{60}Co) are included as unconstrained free parameters. The relative contributions of $0\nu\beta\beta$ window backgrounds are additionally constrained by the time variation of the event rate in the energy range $2.2\ \mathrm{MeV} < E < 3.0\ \mathrm{MeV}$.

Fig. 4 shows the resulting best-fit spectral decomposition. $2\nu\beta\beta$ decay is the dominant spectral feature in the low energy region. The best-fit number of ^{136}Xe $2\nu\beta\beta$ decays is $(3.55 \pm 0.03) \times 10^4$, corresponding to an event rate of 80.9 ± 0.7 (ton·day)$^{-1}$. The dominant backgrounds at low energy are from ^{85}Kr and ^{210}Bi, with best-fit rates of 196 ± 8 (ton·day)$^{-1}$and 103 ± 3 (ton·day)$^{-1}$, respectively. The fit yields the following 90% C.L. upper limits on other background rates (per ton·day) in the Xe-LS: ^{40}K <9.6, ^{234}Pa<1.5, ^{134}Cs<0.4, ^{228}Ac <0.7, ^{90}Y < 0.8 and

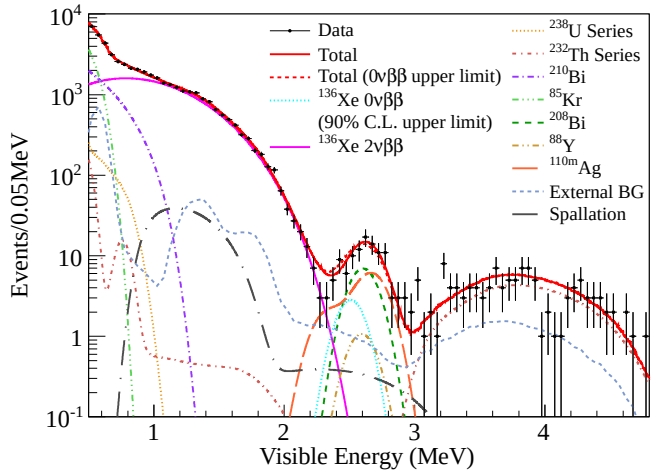

FIG. 4: Energy spectrum of selected $\beta\beta$ decay candidates together with the best-fit backgrounds and $2\nu\beta\beta$ decays, and the 90% C.L. upper limit for $0\nu\beta\beta$ decays.

^{137}Cs<1.1; other fallout isotopes are negligible.

In the $0\nu\beta\beta$ window, a strong peak appears, but the peak is centered significantly above the Q-value of the decay: the hypothesis that the peak can be described by $0\nu\beta\beta$ decay alone is rejected by a χ^2-test at more than 5σ C.L. The best-fit combined background rate in the $0\nu\beta\beta$ window allowing for contributions from $^{110\mathrm{m}}$Ag, ^{88}Y, ^{208}Bi, and ^{60}Co is 0.22 ± 0.04 (ton·day)$^{-1}$. The 90% C.L upper limit on the number of ^{136}Xe $0\nu\beta\beta$ decays is < 15 events, an event rate of < 0.034 (ton·day)$^{-1}$.

The measured $2\nu\beta\beta$ decay half-life of ^{136}Xe is $T^{2\nu}_{1/2} = 2.38 \pm 0.02(\mathrm{stat}) \pm 0.14(\mathrm{syst}) \times 10^{21}$ yr. This is consistent with the result obtained by EXO-200, $T^{2\nu}_{1/2} = 2.11 \pm 0.04(\mathrm{stat}) \pm 0.21(\mathrm{syst}) \times 10^{21}$ yr [5]. For $0\nu\beta\beta$ decay, the data give a lower limit of $T^{0\nu}_{1/2} > 5.7 \times 10^{24}$ yr (90% C.L.), which corresponds to almost a five-fold improvement over previous limits [6]. From the limit on the ^{136}Xe $0\nu\beta\beta$ decay half-life we obtain a 90% C.L. upper limit of $\langle m_{\beta\beta} \rangle < (0.3 - 0.6)$ eV using recent QRPA (CCM SRC) [15] and shell model [16] nuclear matrix elements calculated prior to the EXO-200 measurement.

In summary, KamLAND-Zen provides an improved measurement of the ^{136}Xe $2\nu\beta\beta$ decay half-life. The result is consistent with that of EXO-200 and supports the conclusion that the directly measured half-life is significantly less than the lower limits reported in earlier experiments. Our analysis includes a search for $0\nu\beta\beta$ decay of ^{136}Xe and yields an improved lower limit on its half-life. Removal of contaminants in the Xe-LS is an important task to improve the $0\nu\beta\beta$ decay search sensitivity. In the future, systematic uncertainties will also be reduced by performing source calibrations in the Xe-LS.

The KamLAND-Zen experiment is supported by the Grant-in-Aid for Specially Promoted Research under grant 21000001 of the Japanese Ministry of Education, Culture, Sports, Science and Technology; the World Premier Inter-

national Research Center Initiative (WPI Initiative), MEXT, Japan; and under the US Department of Energy (DOE) Grant No. DE-AC02-05CH11231, as well as other DOE grants to individual institutions. The Kamioka Mining and Smelting Company has provided service for activities in the mine.

[1] J. Schechter and J. W. F. Valle, Phys. Rev. D **25**, 2951 (1982).
[2] K. Nakamura *et al.*, (Particle Data Group), J. Phys. G **37** (2010).
[3] V. A. Rodin, A. Faessler, F. Šimkovic, and P. Vogel, Phys. Rev. C **68**, 044302 (2003).
[4] F. Šimkovic, A. Faessler, V. Rodin, P. Vogel, and J. Engel, Phys. Rev. C **77**, 045503 (2008).
[5] N. Ackerman *et al.*, (EXO Collaboration), Phys. Rev. Lett. **107**, 212501 (2011).
[6] R. Bernabei *et al.*, Phys. Lett. B **546**, 23 (2002).
[7] J. Gavriljuk, A. Gangapshev, V. Kuzminov, S. Panasenko, and S. Ratkevich, Phys. At. Nucl. **69**, 2129 (2006).
[8] S. Abe *et al.*, (KamLAND Collaboration), Phys. Rev. C **81**, 025807 (2010).
[9] M. Redshaw, E. Wingfield, J. McDaniel, and E. G. Myers, Phys. Rev. Lett. **98**, 053003 (2007).
[10] S. Abe *et al.*, (KamLAND Collaboration), Phys. Rev. C **84**, 035804 (2011).
[11] R. S. Raghavan, Phys. Rev. Lett. **72**, 1411 (1994).
[12] ENSDF, the Evaluated Nuclear Structure Data File available at http://ie.lbl.gov/databases/ensdfserve.html (2006).
[13] P. Napolitani *et al.*, Phys. Rev. C **76**, 064609 (2007).
[14] W. C. Haxton and G. J. Stephenson Jr., Prog. Part. Nucl. Phys. **12**, 409 (1984).
[15] F. Šimkovic, A. Faessler, H. Müther, V. Rodin, and M. Stauf, Phys. Rev. C **79**, 055501 (2009).
[16] J. Menéndez, A. Poves, E. Caurier, and F. Nowacki, Nucl. Phys. A **818**, 139 (2009).